VOLUME 7, NUMBER 3, MARCH 2007

NANO LETTERS

Atomistic Modeling of Multilayered Ceria Nanotubes

Paul Martin,[†] Stephen C. Parker,*[,†] Dean C. Sayle,[‡] and Graeme W. Watson[§]

Department of Chemistry, University of Bath, Claverton Down, Bath, Avon, U.K., DMAS, Cranfield University, Shrivenham, Swindon, U.K., and School of Chemistry, Trinity College, Dublin 2, Ireland

Received November 15, 2006; Revised Manuscript Received January 30, 2007

ABSTRACT

Ceria has become a very important material for catalytic applications. Many applications take advantage of its high oxygen storage capacity (OSC). We propose a new polycrystalline multilayered nanotube structure that could go some way to further unlocking the oxygen storage capabilities of the material. We illustrate how our simulation models are constructed and further investigate the potential reactivity of the new structure, by comparing predictions of vacancy cluster segregation behavior to that predicted for the most stable flat {111} surface.

Materials based on ceria (CeO_{2-x}) are used in the production and purification of hydrogen, the purification of exhaust gases in three-way automotive catalytic converters, solid-oxide fuel cell technology, and other catalytic applications.[1−4]

The reason for the success of ceria in these applications is its abilities to shift between its two oxidation states, Ce(III) and Ce(IV), and to utilize oxygen to react with hydrocarbons, carbon monoxide, and nitrogen monoxide. All of these applications make use of these electrochemical properties. The ability of ceria to stabilize surface oxygen vacancies in conjunction with high oxygen mobility through the lattice thus allows ceria to behave as an oxygen buffer and remains central to the effectiveness of the catalyst.

One way of enhancing the oxygen mobility is to modify the particle size and shape. Recent experimental work[5] suggests that it is now possible to synthesize ceria nanotubes. Clearly it is important to investigate the extent to which the key properties of ceria are affected by being prepared as a nanotube.

In this paper, we begin to address this question using modern computational techniques because, although possible, the nanotubes are very difficult to synthesize and moreover their surfaces are very difficult to characterize. In this work, we attempt to characterize ceria nanotube surfaces and investigate potential differences between ceria nanotube structure and the most stable[6] {111} flat surface by the modeling and simulation of oxygen vacancy formation and segregation in the ceria nanotubes and comparing this to that predicted for the flat {111} surface.

Atomistic simulation techniques based on the Born model[7] of solids were employed for the simulation calculations. The model assumes full ionic charges for the cerium and oxygen atoms and parametrized analytical functions to describe the repulsion between the electronic charge clouds and the van der Waals attractions between all species in the crystal. The

* s.c.parker@bath.ac.uk.
† University of Bath.
‡ University of Cranfield.
§ Trinity College.

10.1021/nl0626737 CCC: $37.00
Published on Web 02/28/2007

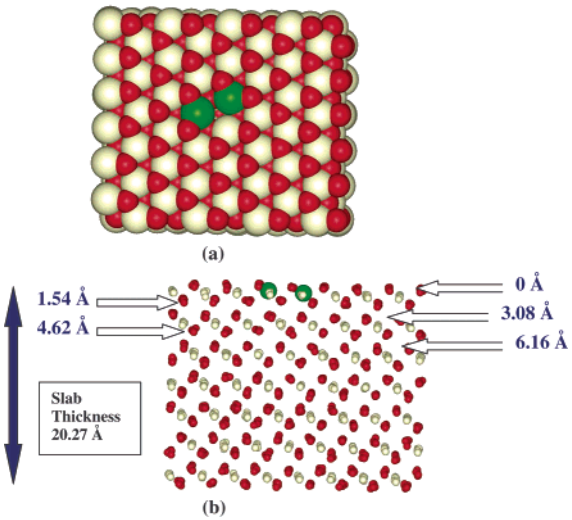

Figure 1. Compensated vacancy cluster in the {111} surface: (a) plan view; (b) side view; green = Ce^{3+}; white = Ce^{4+}; red = O^{2-}.

parameters of the potential model used in this work were derived by Balducci et al.[8] and are a minor modification of a potential derived by Sayle et al.[9] A further feature of the model is the inclusion of the shell model of Dick and Overhauser[10] to simulate ionic polarizability of the oxygen ions. In this model, the oxygen ion is represented as a core plus a shell coupled by a harmonic spring. The total charge (−2 for oxygen) is distributed between the shell and the core. In the molecular dynamics (MD) simulations, the shells were given a mass of 0.5 au, and an *NVT* (constant number of atoms, volume, and temperature) ensemble was used.

MD simulations were first used to calculate the defect formation energy of a charge compensated oxygen vacancy in a simulated slab of {111} surface ceria as a function of depth from the surface. This will enable us to assess how a charge compensated oxygen vacancy might segregate to the stable {111} surface of ceria. In the model presented here, the mode of charge compensation for the oxygen vacancies is the substitution of two trivalent Ce^{3+} cations for two Ce^{4+}. It is important to note that a number of ab initio studies, for example, Watson et al.,[11−14] have been performed on ceria. Comparison between the ab initio and potential based approaches used here, see, for example, ref 15, and comparisons with experimental work[16] have shown that the potentials are reliable and the local model is justified

The simulation slab is approximately 20 Å thick, this allows the bulk material to be simulated at the center of the slab. Figure 1a shows the charge compensated vacancy cluster in the {111} surface, and Figure 1b illustrates how we move the vacancy cluster stepwise to different depths toward the center of the slab. It is also possible to investigate vacancy cluster segregation to the surface using MD. This is achieved by carrying out a series of vacancy cluster formation energy calculations similar to those developed by Duffy et al.[17−20] First, the energy of the stoichiometric surface slab is calculated, which is defined as the thermally averaged sum of the interaction energies between all atoms in slab. This is followed by the calculation of the energy of a defective slab, that is, one containing a vacancy cluster. The

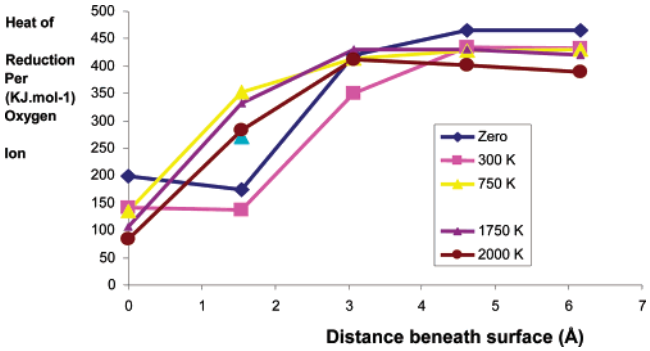

Figure 2. Heats of reduction for vacancy versus distance beneath {111} surface at a range of temperatures.

difference between this energy and the energy of the original stoichiometric slab gives the defect formation energy of the charge compensated vacancy cluster at that particular distance from the surface. A more useful quantity for comparison with experiment is the heat of reduction where oxygen is removed as gaseous oxygen and two adjacent Ce(IV) ions are reduced to Ce(III). However, because we have used an ionic model, we are required to add a correction consisting of the oxygen electron affinities, bond formation, and cerium's fourth ionization potential. Because these are not particularly well-constrained experimentally, we evaluated the correction by taking the difference between the experimental[21] and simulated values for the following reaction:

$$2CeO_2 \rightarrow Ce_2O_3 + \frac{1}{2}O_2$$

Figure 2 shows the calculated heat of reduction as a function of depth and at different temperatures.

At low temperatures, the vacancy cluster is most stable just underneath the {111} surface, but at elevated temperatures, the vacancy cluster segregates to the surface. The next stage is to compare the heats of reduction at the surface, which give rise to the oxygen vacancies with the heat of reduction of a ceria nanotube. However, before discussing that we briefly summarize the method for constructing a wrapped nanotube.

The approach for constructing a multilayered wrapped nanotube is summarized in Figure 3. The basic approach is to construct a finite strip of a multilayered slab, which is then wrapped around to make the tube, and then the outer layers are repackaged to release the strain. Once the tube is constructed, we anneal the simulation cell using molecular dynamics at a variety of temperatures until the energy and structure were invariant.

This methodology has been used to generate various different sized models for an array of different materials. We next focused on a nanotube model, similar in size to that prepared experimentally.[5]

A multilayered simulation model was constructed that contained 8758 CeO_2 units. The model was relaxed using molecular dynamics simulation at 300 K for a simulation time of 1 ns. The tube had a wall thickness of 5.5 nm and a lumen diameter of 4.8 nm. Figure 4 shows a cut through the nanotube. From this figure, it is evident that the outer surfaces

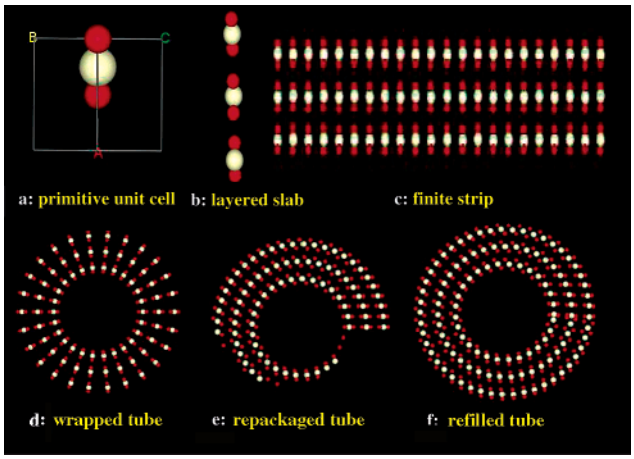

Figure 3. The wrapping method. This method involves six construction steps (steps a−f). A primitive unit cell of CeO_2 (a) is converted to a multilayered slab (b), which is periodic in the *Y* and *Z* directions. A finite strip of this slab (c) is constructed along the *Y* direction, which is then wrapped around to make the tube (d), which is now periodic in the *Z* direction. The tube (d) has a large amount of strain on the outer edges; this strain is removed by repackaging the outer regions (e) to maintain bond distances around the tube, and step f is where additional atoms are added to complete the tube.

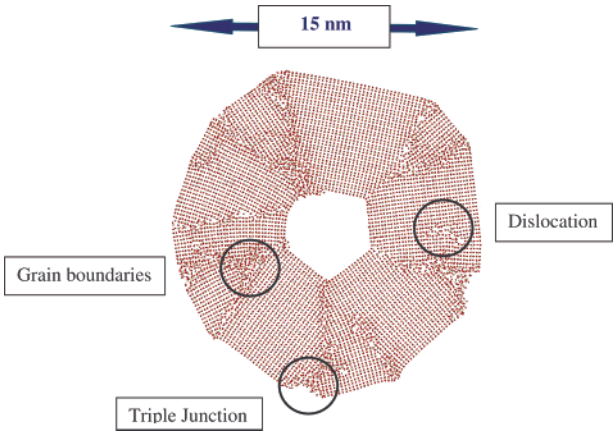

Figure 4. Multilayer wrapped nanotube model showing polycrystalline behavior. The figure indicates important structural features including boundaries, junctions, and dislocations.

have remained largely smooth {111}. Clearly, the strain is accommodated by the introduction of grain boundaries and dislocations. Because these have formed naturally with the simulation, they represent a useful source of extended defects to the model.

We first investigated the stability of a charge compensated vacancy at different positions within the nanotube structure these included at the inner and outer surfaces and at the grain boundaries. Once the vacancy cluster is introduced at a particular position the simulation is relaxed for 50 ps. The energy is monitored to ensure that it is converged. As with the defective {111} surface calculations, the difference between this energy and the original total energy of the stoichiometric tube gives the defect energy of the vacancy cluster at that particular position within the polycrystalline nanotube model. It is therefore now possible to model how a vacancy cluster might segregate to the surfaces and even

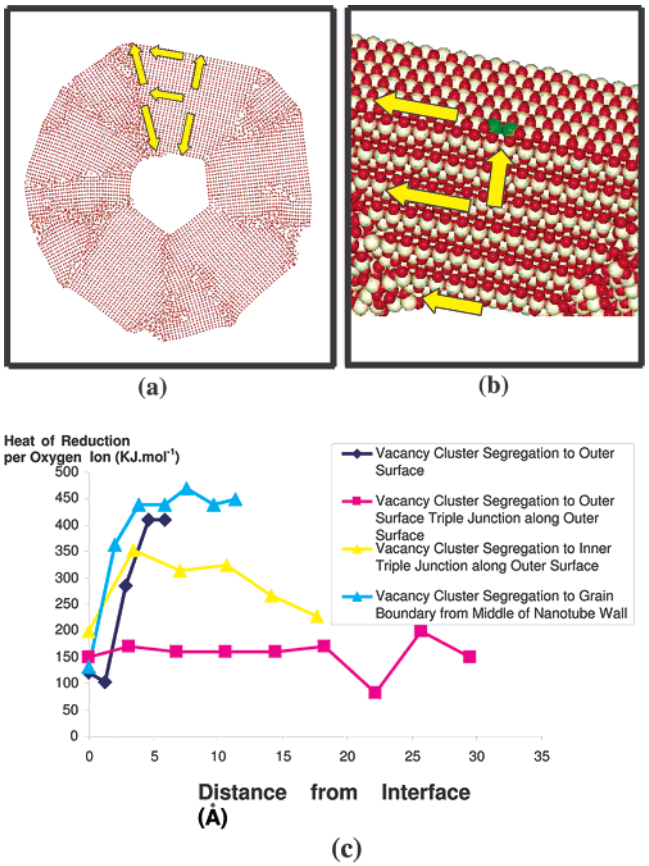

Figure 5. Panels a and b show the locations of the vacancy clusters and panel c shows the predicted heats of reduction for vacancies within the polycrystalline nanotube structure.

along different portions of the surfaces, as well as to grain boundaries, triple junctions, and even individual dislocations, from inside the nanotube structure (Figure 5a,b). We then compare these models of vacancy cluster segregation behavior to that predicted for the most stable flat {111} surface. We now highlight some interesting comparisons.

Figure 5c shows that, similar to the defective {111} surface predictions at low temperature, the vacancy cluster is more stable just under the outer surface of the nanotube. A similar energetic barrier exists for the vacancy cluster to segregate to the outer surface as there is for the cluster to segregate to the stable {111} surface, although this energetic barrier to surface segregation disappears at elevated temperatures. Importantly, the enthalpy of reduction in forming the charge compensated oxygen vacancy is 121.0 kJ·mol^{-1} at the outer surface of the nanotube compared with 199.2 kJ·mol^{-1} on the {111} surface. The vacancy cluster is estimated to be 78 kJ·mol^{-1} more stable at the nanotube outer surface than at the stable {111} flat surface.

The plot describing vacancy cluster segregation to the outer surface triple junction, along the outer surface, predicts a relatively more stable vacancy cluster at the triple junction. The defect formation energy increases slightly as the cluster is placed further away from the outer triple junction along the outer nanotube surface. An anomaly exists at the position about 22 Å along the surface, away from the triple junction, where a very stable vacancy cluster is predicted. The vacancy cluster positions on the outer surface are all predicted to be

more stable compared with positions under the surface. The inner nanotube surface triple junction position is also predicted to have a relatively stable vacancy cluster position compared with other inner surface positions. However, vacancies adjacent to the triple junction (up to 3−4 Å) are predicted to be about 100−150 kJ·mol^{-1} less stable but increase in stability from about 3−4 Å away from this adjacent position. At positions of about 15 Å away from the inner triple junction, the vacancy cluster stability becomes similar to that at the triple junction position.

The plot also allows predictions of how much more stable the vacancy cluster is at the grain boundaries compared with positions adjacent to it and positions deeper toward the nanotube center. At the grain-boundary position at the center of the nanotube wall, the enthalpy of reduction is predicted to be 63.2 kJ·mol^{-1}, while an adjacent vacancy position is 121.0 kJ·mol^{-1}, and slightly further into the bulk of the nanotube wall, it is 400.8 kJ·mol^{-1}. These calculations predict that vacancy clusters will segregate toward these grain boundaries. The defect cluster is 57.8 kJ·mol^{-1} more stable at the grain boundary compared with the adjacent deeper position but 279.8 kJ·mol^{-1} more stable when compared with positions between 5 and 10 Å deeper into the nanotube structure. There is no thermodynamic barrier to vacancy cluster segregation to the grain boundary.

In conclusion, these nanotube models predict a polycrystalline multilayered nanotube structure with highly enhanced stabilization of oxygen vacancies at surfaces, grain boundaries, and triple junctions. These defects are potential reaction sites, so the structure represents a new nanostructure that, combined with its inherent high surface area to bulk ratio, should have enhanced activity, which would unlock the oxygen storage capabilities of ceria.

Acknowledgment. We thank the Engineering and Physical Sciences Research Council (EPSRC) in the United Kingdom for Funding Grants GR/S48448/01 and GR/S84415/01.

References

(1) Deluga, G. A.; Salge, J. R.; Schmidt, L. D.; Verykios, X. E. *Science* **2004**, *303*, 993.
(2) Otsuka, K.; Ushiyama, T.; Yamanaka, I. *Chem. Lett*. **1993**, *9*, 1517.
(3) Trovarelli, A., Ed. *Catalysis by Ceria and Related Materials*; Imperial College Press: London, 2002.
(4) Park, S.; Vohs, J. M.; Gorte, R. J. *Nature* **2000**, *404*, 265.
(5) Han, W. Q.; Wu, L. J.; Zhu, Y. M. *J. Am. Chem. Soc.* **2005**, *127*, 12814.
(6) Nolan, M.; Grigoleit, S.; Sayle, D. C.; Parker, S. C.; Watson, G. W. *Surf. Sci.* **2005**, *576*, 217.
(7) Born, M.; Mayer, J. E. *Z. Phys.* **1932**, *75*, 1.
(8) Balducci, G.; Kaspar, J.; Fornasiero, P.; Graziani, M.; Islam, M. S.; Gale, J. D. *J. Phys. Chem. B* **1997**, *101*, 10.
(9) Sayle, T. X. T.; Parker, S. C.; Catlow, C. R. A. *J. Phys. Chem.* **1994**, *98*, 13625.
(10) Dick, B. G.; Overhauser, A. W. *Phys. Rev.* **1958**, *112*, 90.
(11) Nolan, M.; Grigoleit, S.; Sayle, D. C.; Parker, S. C.; Watson, G. W. *Surf. Sci.* **2005**, *576*, 217.
(12) Nolan, M.; Parker, S. C.; Watson, G. W. *Surf. Sci.* **2005**, *595*, 223.
(13) Nolan, M.; Parker, S. C.; Watson, G. W. *J. Phys. Chem. B* **2006**, *110*, 2256.
(14) Nolan, M.; Parker, S. C.; Watson, G. W. *Phys. Chem. Chem. Phys.* **2006**, *8*, 216.
(15) Parker, S. C.; Kerisit, S.; Marmier, A.; Grigoleit, S.; Watson, G. W. *Faraday Discuss.* **2003**, 124.
(16) Pfau, A.; Schierbaum, K. D. *Surf. Sci.* **1994**, *321*, 71.
(17) Duffy, D. M.; Hoare, J. P.; Tasker, P. W. *J. Phys. C* **1984**, *17*, L195.
(18) Duffy, D. M.; Tasker, P. W. *J. Appl. Phys.* **1984**, *56*, 971.
(19) Duffy, D. M.; Tasker, P. W. *Philos. Mag. A* **1984**, *50*, 143.
(20) Duffy, D. M.; Tasker, P. W. *Philos. Mag. A* **1984**, *50*, 155.
(21) Weast, R. C.; Astle, M. J. *Handbook of Physical Chemistry*, 61st ed.; CRC Press, Inc.: Boca Raton, FL, 1980−1981.

NL0626737